

NMR investigation of spin flip phase transitions in yttrium-terbium iron garnets

V. A. Borodin, V. D. Doroshev, V. A. Klochan, N. M. Kovtun, R. Z. Levitin, and A. S. Markosyan

Donets Physico-technical Institute, Ukrainian Academy of Sciences

(Submitted October 8, 1975)

Zh. Eksp. Teor. Fiz. 70, 1363-1378 (April 1976)

The spin flip transition induced by temperature in iron garnet single crystals $Tb_xY_{3-x}Fe_5O_{12}$ ($x = 0.10, 0.26, 0.50$) in a zero magnetic field is studied by the NMR technique for Fe^{57} . It is found that in the multidomain state of the specimens the reorientation of the spins from crystallographic directions of the $\langle 100 \rangle$ type to directions $\langle 111 \rangle$ is a first-order transition. The transition exhibits no temperature hysteresis, and magnetic phase coexistence is observed in the neighborhood of the transitions. The measured transition temperatures are in good agreement with the phase diagram based on the experimental values of the magnetic anisotropy constants $K_1(T)$ and $K_2(T)$. The cited singularities of the spin reorientation are consistent with the theoretical model proposed for orientation spin transitions in the multidomain state of cubic ferromagnets by Belov, Zvezdin *et al.* (1975). The temperature range of magnetic phase coexistence is estimated theoretically within the framework of the model.

PACS numbers: 76.60.-k, 75.25.+z

1. INTRODUCTION

Much attention has been paid recently to the study of orientational phase transitions—one of the modifications of magnetic transitions of the order-order type. Of definite interest here are temperature transitions in a zero magnetic field, when the change in the character of the magnetic crystallographic anisotropy changes the direction of the magnetic moments relative to the symmetry axis of the crystal (without a significant change in the values of the moments) either jumpwise (first-order transitions) or in a continuous manner (second-order transitions). It can be noted that up to now the spin-flip (SF) transitions in temperature have been intensely investigated principally in magnetic crystals, the behavior of which fits satisfactorily in the framework of uniaxial anisotropic interactions, viz., in hexagonal cobalt, $Mn_{2-x}Cr_xSb$, hematite, rare-earth orthoferrites, etc. At the same time there are only a few theoretical and experimental papers devoted to SF transitions in cubic crystals (e.g., ^[1,2]), although there is an appreciable number of cubic magnets that experience SF transitions.

The changes of the easy magnetization axes in cubic ferromagnets and ferrimagnets were analyzed in^[1] from the point of view of the theory of SF phase transitions. It turned out that the character of the spin flip changes significantly, depending on whether the sample is single-domain, i.e., magnetically homogeneous, or whether it has inhomogeneities in the form of a domain structure. In the single-domain state, the SF transitions are of first order and should experience hysteresis. Allowance for the domain structure of bulky samples, as shown by a theoretical analysis, eliminates the temperature hysteresis of these transitions, and different magnetic phases should coexist in a certain temperature interval.

Yttrium-terbium iron garnets turned out to be a convenient object for an experimental verification of the

deductions of the theory, with the SF phase transition $\Phi\langle 100 \rangle \rightleftharpoons \Phi\langle 111 \rangle$ as an example. It was shown in^[1] that the theoretical orientational phase diagram of these ferrites is in good agreement with the experimental diagram reconstructed from measurements of the torques, and the presence of hysteresis of the spin flip in the single-domain state was unambiguously established. In the multidomain state (zero magnetic field), the SF transition was detected indirectly, by means of the anomalies of Young's modulus and of the initial magnetic susceptibility; it was assumed that in accordance with the theoretical analysis the SF transition temperature corresponds to a maximum of the initial susceptibility and a minimum of Young's modulus. The temperature dependences of the initial susceptibility and of Young's modulus had no hysteresis, and this confirmed indirectly the theoretical conclusion that the transition in multidomain crystals is not subject to hysteresis.

We present here the results of a study of SF phase transitions in single-crystal iron garnets $Tb_xY_{3-x}Fe_5O_{12}$ ($x = 0.10; 0.26; 0.50$) by the method of NMR of Fe^{57} , using the torque measurement data. Just as in the study of the SF transition in a lithium-cobalt ferrite with spinel structure,^[2] in the case of the yttrium-terbium iron garnets the NMR procedure has made it possible to determine the distribution of the magnetization in the volume of bulky multidomain samples of cubic ferrimagnets. As a result, the character of the transition $\Phi\langle 100 \rangle \rightleftharpoons \Phi\langle 111 \rangle$ in the multidomain state was unambiguously established; the temperatures of the SF transitions in a zero magnetic field were determined by a direct procedure and compared with the values corresponding to the theoretical phase diagram; coexistence of magnetic phases was observed and experimental temperature dependences were obtained for the volumes of the coexisting phases, and were compared with the theoretical relations. All these data supplement substantially the results obtained by traditional methods.

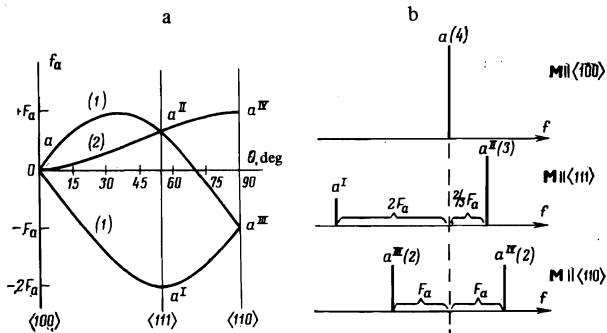


FIG. 1. Resonant frequency and spectra of NMR octahedral Fe^{3+} ions in iron garnets. a) Theoretical angular dependence of the anisotropic components of the resonant frequencies for the non-equivalent a -ions in the unit cell. The magnetization lies in a plane of type $\{110\}$; θ is the angle between \mathbf{M} and the $\langle 100 \rangle$ direction. b) Theoretical NMR spectra for three possible types of domains. The dashed line shows the position of the isotropic component of the resonant frequency. The quantities in the parentheses are the relative intensities of the resonance lines.

2. EXPERIMENTAL PROCEDURE, APPARATUS, AND SAMPLES

The distribution of the magnetization in domains of ferrites with garnet structure (space group $Ia\bar{3}d$) by the NMR method is made possible by the fact that the local symmetry of the surrounding of the Fe^{3+} ions in octahedral (a) and tetrahedral (d) sites is lower than cubic (even though the crystal as a whole is cubic), and consequently there are anisotropic components of the local magnetic fields at the nuclei of these ions; these components carry information on the direction of the magnetization in the crystal. Thus, the a -ions in the unit cell are divided into four non-equivalent groups in accordance with the four possible directions of the local threefold axes of the type $\langle 111 \rangle$. In exactly the same way, the d -ions form three non-equivalent groups that differ in the directions of the local inversion fourfold axes of the type $\langle 100 \rangle$.

According to the theoretical concepts^[3] and the experimental data,^[4] the demagnetizing fields at the nuclei in the interior of the domains of multidomain iron-garnet samples are negligible in size. There are therefore only two anisotropic components of the local field at the nucleus, the dipole field \mathbf{H}_{dip} produced by the neighboring magnetic ions, and the anisotropic hyperfine field \mathbf{H}_{an} due to the deviation of the symmetry of the wave functions of the Fe^{3+} ions from cubic in the low-symmetry crystal fields.^[3] In the interpretation of the anisotropic effects in NMR spectra in first-order approximation we may take into account only the projections of the anisotropic fields on the direction of the isotropic hyperfine field (the z axis), since the isotropic field resulting from the polarization of the s shells of the ionic core by the intrinsic spin of the Fe^{3+} ion exceeds by two orders of magnitude the anisotropic components ($H_n \sim 500$ kOe). For the indicated symmetry of the a -sites and d -sites, \mathbf{H}_{dip} and \mathbf{H}_n are axially symmetrical,^[5] and their sum can be written in the form

$$|H_{\text{loc}}| = (3 \cos^2 \alpha - 1) \{H_{\text{dip}}^z + H_{\text{an}}^z\}$$

$$= (3 \cos^2 \alpha - 1) \left\{ \sum_{i=1}^4 \frac{1}{2} \left(\frac{3 \cos^2 \alpha_i - 1}{r_i^3} \right) \mu_i + H_{\text{an}}^z \right\}. \quad (1)$$

Here H_{dip}^z is calculated in the model of pointlike dipoles for a collinear magnetic structure; account is taken of the fact the isotropic hyperfine field \mathbf{H}_n is antiparallel to the sublattice magnetization. α is the angle between the local symmetry axis of the site and the resultant magnetization, r_i is the radius vector of the i -th ion, μ_i is the magnetic moment of this ion, and α_i is the angle between r_i and the local axis.

In the three-sublattice model of the iron garnet, the dipole lattice sums reduce to the following simple expression^[4]:

$$H_{\text{dip}}^z = \begin{cases} A \left[\sigma_a + \frac{M_{0c}}{M_{0d}} \sigma_c \right] & (a\text{-sites}), \\ A \left[0.29\sigma_a - 0.21\sigma_d - 1.03 \frac{M_{0c}}{M_{0d}} \sigma_c \right] & (d\text{-sites}), \end{cases} \quad (2)$$

where σ_a , σ_d , and σ_c are the relative magnetizations of the a -, d -, and c sublattices at a given temperature, while M_{0c} and M_{0d} are the magnetizations of the c and d sublattices at 0°K . The calculated value of A for $\mu_a = \mu_d = 5\mu_B$ and for the lattice parameter $a = 12.376 \text{ \AA}$ (yttrium iron garnet) amounts to 2044 Oe. It is obvious that at small terbium concentrations ($x \leq 0.5$) and relatively high temperatures (100–150 °K) the contributions to the dipole fields from the rare-earth sublattice are small in our case (terms proportional to σ_c). Then the dipole fields at the nuclei of the d ions will be much smaller than the dipole fields at the nuclei of the a ions, in view of the almost neutral cancellation of the contributions from the a and d sublattices. The same relation obtained also between the experimental values of the fields H_{an} ,^[4] which do not lend themselves to a sufficiently accurate calculation.^[5] For example, for yttrium iron garnet^[4] the experimental summary values of the anisotropic components of the local field at the nucleus are the following:

$$H_{\text{dip}}^z + H_{\text{an}}^z = \begin{cases} 2730 \text{ Oe} & (a\text{-sites}) \\ 345 \text{ Oe} & (d\text{-sites}) \end{cases}$$

Therefore, from the experimental point of view, to study the distribution of the magnetization in the iron-garnet domains is preferable to register the spectra of the octahedral Fe^{3+} ions. Changing over to anisotropic components of the resonant frequency of the a ions, we can write

$$f_a^{(k)} = -(3 \cos^2 \alpha_k - 1) F_a,$$

where $F_a = (\gamma_n/2\pi) \{H_{\text{dip}}^z + H_{\text{an}}^z\}$, $\gamma_n/2\pi = 137.4 \text{ Hz/Oe}$; α_k are the angles between the magnetization direction in the domain and the local symmetry axes of type $\langle 111 \rangle$ of the a ions, and $k = 1, \dots, 4$.

At an arbitrary direction of the magnetization in the domain, four resonance lines should be observed, inasmuch, as already indicated, there are four types of none-equivalent a -ions that differ in the spatial disposition of the local axes. It is convenient to trace the variation of the structure of the NMR spectrum if the magnetization \mathbf{M} rotates in a plane of the $\{110\}$ type, which contains all the principal directions of the cubic

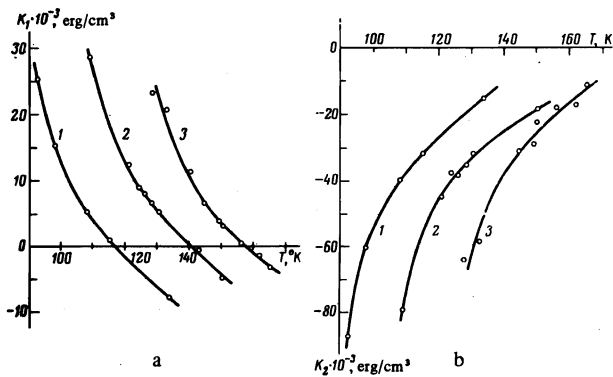


FIG. 2. Temperature dependence of the first magnetic-anisotropy constant K_1 (a) and of the second constant K_2 (b) of yttrium-terbium iron garnets. 1) $x=0.10$; 2) $x=0.26$; 3) $x=0.50$.

crystal. In this case there is partial degeneracy and three branches of the resonant frequency should be observed, as shown in Fig. 1a. It is clearly seen that the magnetization directions along the principal axes correspond to spectra (Fig. 1b) that differ in the number of the lines, in their positions, and in their intensities. This makes it possible to determine from the form of the spectrum the equilibrium directions of the magnetization in the domains. Depending on the type of the SF phase transition, the spectra should be transformed in different manners. If a SF transition of the second kind is realized, for example from a direction of the type (100) to a direction (111) in the {110} plane, then a single resonance line (line a in the phase $\Phi\langle 100 \rangle$, Fig. 1) should split smoothly into three lines ("canted phase") with an intensity ratio 1:2:1, two of which then coalesce, and in the phase $\Phi\langle 111 \rangle$ the spectrum will consist of two lines with an intensity ratio 1:3 (lines a^I and a^{II} , Fig. 1). If the spin flip is a first-order phase transition, then no continuous transitions in frequency between the spectra of the phases $\Phi\langle 100 \rangle$ and $\Phi\langle 111 \rangle$ should take place.¹⁾

We note that, in contrast to most methods in which either surface domains or domains in thin plates are studied, the NMR procedure makes it possible to investigate volume domain structures of bulky sample.

The NMR spectra were registered by Hahn's two-pulse spin-echo method with the aid of a semi-automatic spectrometer equipped with a stroboscopic integrator. The spectrum is the amplitude of the spin-echo signal, recorded on the chart of an automatic potentiometer as a function of the carrier frequency of the excited pulses. To distinguish between the NMR signals from the nuclei in the volume of the domains and the signals from the nuclei in the domain walls, use was made of the differences between the NMR gain η , the relaxation times T_1 and T_2 , and the width of the spin-echo signals. The necessary resolution of the spectrometer was attained by using exciting pulses of long duration (5–20 μsec). The samples were cooled by an electronically temperature-stabilized stream of nitrogen vapor; the accuracy of the sample-temperature stabilization was not worse than $\pm 0.1^\circ\text{K}$.

The magnetic anisotropic constants were measured by the torque method in fields up to 8 kOe. The samples were single-crystal spheres with approximate diameter of 3 mm, oriented in the {110} plane. We used a frequency-inductive method of measuring the rotation angle of the moving system of the anisometer. The thicknesses of the interchangeable elastic elements were chosen such that maximum rotation angle did not exceed $0.2\text{--}0.5^\circ$. Angles of this magnitude can be disregarded in the reduction of the torque curves, since they are of the order of the error in the angles between the direction of the magnetic field and the crystallographic axes. The anisometer was calibrated against the torque of a current-carrying loop with known geometric dimensions. The torque measurement accuracy was not worse than $\pm 5\%$.

Single-crystal ferrites of the system $\text{Tb}_x\text{Y}_{3-x}\text{Fe}_5\text{O}_{12}$ ($x=0.10$; 0.26; 0.50) were grown by the method of spontaneous crystallization from the melt. The methods used to grow the crystal and to monitor the composition are described in^[7,8]. To decrease the uniaxial growth anisotropy, the samples were annealed at 1300°C for 24 hours in air. In the NMR measurements we used a solitary untreated single crystals with natural faceting and with linear dimensions 1–2 cm. The spheres used for the measurements of the magnetic-anisotropy constants were made from the same single crystals after the performance of the NMR measurements.

3. EXPERIMENTAL RESULTS AND THE DISCUSSION

We have previously observed^[7] the reversal of the sign of the first magnetic-anisotropy constant K_1 of yttrium-terbium iron garnets ($x \leq 2.12$) with changing temperature, which leads to a temperature SF phase transition in these ferrites. This behavior of $K_1(T)$ is due to the fact that the contribution made to K_1 by the Tb^{3+} ions in substituted yttrium-terbium iron garnets has a positive sign, and that from Fe^{3+} ions has a negative sign. At high temperatures, the magnetic anisotropy of the iron garnets is determined almost exclusively by the iron sublattices, and therefore the constant K_1 is negative, but with decreasing temperature the contribution of the rare-earth sublattice increases abruptly and at a certain temperature, which depends on the terbium concentration, the contributions made to the first anisotropy come from the terbium and iron ions are cancelled out.

Figure 2 shows the measured anisotropy constants $K_1(T)$ and $K_2(T)$ of crystals with terbium concentration $x=0.10$, 0.26, and 0.50. These measurements were made near the temperatures of the compensation of the constant K_1 , and were performed in greater detail than in^[7], for the purpose of a more accurate determination of the phase-transition temperatures. It must also be noted that there are no data in^[7] for the ferrite with $x=0.10$. The cited temperature dependences of the anisotropy constants were obtained as a result of measurements of the torques in a magnetic field of 5 kOe. Control measurements in the range of fields 2–8 kOe have shown that at the relatively high temperatures

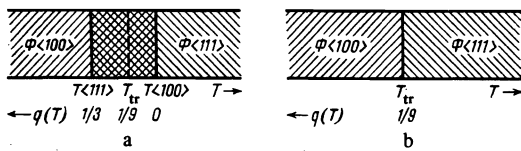


FIG. 3. Phase diagram of the temperature SF transition $\Phi\langle 100 \rangle \rightleftharpoons \Phi\langle 111 \rangle$. $q = K_1/|K_2|$; $K_2 < 0$. a) Single-domain sample, b) multidomain sample.

(110–160°K) and low terbium concentration ($0.10 \leq x \leq 0.50$) of interest to us the dependence of the anisotropy constants on the magnetic field,^[7,9] due to the influence of the external field on the magnetization of the rare-earth sublattice, is weakly pronounced. Therefore the results presented in Fig. 2 differ insignificantly from the data obtained by extrapolation to a zero magnetic field. It follows from the presented dependences that the first anisotropy constant K_1 goes through zero at temperatures 117, 141, and 158°K for the ferrites with terbium concentration $x = 0.10, 0.26,$ and 0.50 , respectively, whereas the constant K_2 remains negative at all temperatures.

The theoretical orientational phase diagram of a cubic ferromagnet or a ferrimagnet admits of three SF phase transitions:

$$\Phi\langle 100 \rangle \rightleftharpoons \Phi\langle 111 \rangle, \quad \Phi\langle 111 \rangle \rightleftharpoons \Phi\langle 110 \rangle \quad \text{and} \quad \Phi\langle 110 \rangle \rightleftharpoons \Phi\langle 100 \rangle.$$

Indeed, in a single-domain crystal situated in a zero magnetic field, when account is taken of the first two terms of fourth and sixth order expansion of the energy density of the cubic magnetic anisotropy F_A in terms of the direction cosines of the magnetization vector \mathbf{M} , only three magnetic phases are realized: $\Phi\langle 100 \rangle$, $\Phi\langle 111 \rangle$ and $\Phi\langle 110 \rangle$, which correspond to the orientation of \mathbf{M} along the high-symmetry crystallographic directions of the type $\langle 100 \rangle$, $\langle 111 \rangle$ and $\langle 110 \rangle$, and the equilibrium "canted" phases cannot exist.^[11] The minima of the free energy correspond to the following relations between the anisotropy constants:

$$\begin{aligned} K_1 &\geq 0, & (\text{phase } \Phi\langle 100 \rangle); \\ K_1 &\leq -1/3 K_2, & (\text{phase } \Phi\langle 111 \rangle); \\ 0 &\geq K_1 \geq -1/2 K_2, & (\text{phase } \Phi\langle 110 \rangle). \end{aligned} \quad (3)$$

The equalities in relations (3) are the equations of the stability-loss lines of the magnetic phases on a phase diagram plotted in coordinates (K_1, K_2) . It is seen that the phase-stability conditions (3) lead to an overlap of the regions in which the phases $\Phi\langle 100 \rangle$ and $\Phi\langle 111 \rangle$ exist, as well as $\Phi\langle 111 \rangle$ and $\Phi\langle 110 \rangle$ on the phase diagram, i. e., there are regions where these phases can coexist in a metastable state. The phase-transition lines are determined from the condition that the free energies of the different magnetic phases be equal:

$$\begin{aligned} K_1 &= -1/3 K_2, K_1 \geq 0, & (\text{transition } \Phi\langle 100 \rangle \rightleftharpoons \Phi\langle 111 \rangle); \\ K_1 &= -1/2 K_2, K_1 \leq 0, & (\text{transition } \Phi\langle 111 \rangle \rightleftharpoons \Phi\langle 110 \rangle); \\ K_1 &= 0, K_2 \geq 0, & (\text{transition } \Phi\langle 110 \rangle \rightleftharpoons \Phi\langle 100 \rangle). \end{aligned} \quad (4)$$

It is characteristic that in the assumed approximation all three SF phase transitions in a cubic single-domain ferromagnet are first-order transitions. In this lies the principal difference between cubic magnets and uniaxial magnets, in which, when two terms of the expansion of F_A are taken into account, it is possible to have also second order SF phase transitions. The transitions $\Phi\langle 100 \rangle \rightleftharpoons \Phi\langle 111 \rangle$ and $\Phi\langle 111 \rangle \rightleftharpoons \Phi\langle 110 \rangle$ in a single-domain cubic crystal should exhibit hysteresis, since each phase can exist in a metastable state beyond the phase transition line and the spin flip takes place via an irreversible change of the orientation of the vector \mathbf{M} . The transition $\Phi\langle 110 \rangle \rightleftharpoons \Phi\langle 100 \rangle$, in the assumed approximation, is a specific hysteresis-free first-order transition, inasmuch as the regions of the existence of the phases $\Phi\langle 110 \rangle$ and $\Phi\langle 100 \rangle$ are contiguous but do not overlap, while the phase-stability-loss lines coincide with the phase-transition line.

It is obvious that, in accordance with the considered diagram, the temperature dependence of the anisotropy constants of yttrium-terbium iron garnets, shown in Fig. 2, should lead to the SF phase transition $\Phi\langle 100 \rangle \rightleftharpoons \Phi\langle 111 \rangle$. It is convenient to consider this transition in terms of temperature, by introducing the parameter $q(T\langle 111 \rangle) = \frac{1}{3}$. The theoretical phase diagram for a one-domain sample is shown for this case schematically in Fig. 3a. The transition temperature T_{tr} corresponds to the value $q(T_{tr}) = \frac{1}{9}$, while the stability-loss temperatures of the low-temperature phase $\Phi\langle 100 \rangle$ and of the high-temperature phase $\Phi\langle 111 \rangle$ correspond to values $q(T\langle 100 \rangle) = 0$ and $q(T\langle 111 \rangle) = \frac{1}{3}$, respectively. The overlap of the phase-coexistence regions is clearly seen, and should lead to a temperature hysteresis of the transition with a maximum loop width equal to the metastable-state interval $(T\langle 100 \rangle - T\langle 111 \rangle)$. Figure 4 shows the temperature dependences of the parameter q of the investigated compositions of the yttrium-terbium iron garnet, while the table lists the temperatures of the transitions and magnetic-phase stability losses, determined from the data of Fig. 4, i. e., from the theoretical phase diagram on the basis of the experimental values of the anisotropy constants $K_1(T)$ and $K_2(T)$.

A one-domain state of bulky samples of finite dimensions can be realized in a saturating magnetic field. To exclude the anisotropy contribution made to the free energy by the anisotropy of the shape of the sample and by the change of the energy of the interaction with the external magnetic field in the spin flip, the experiments on the temperature SF transitions in the single-domain state were carried out on samples in the form of disks suspended on filaments, the elasticity of which could be neglected. Information on the change of the direc-

tion of F_A are taken into account, it is possible to have also second order SF phase transitions. The transitions $\Phi\langle 100 \rangle \rightleftharpoons \Phi\langle 111 \rangle$ and $\Phi\langle 111 \rangle \rightleftharpoons \Phi\langle 110 \rangle$ in a single-domain cubic crystal should exhibit hysteresis, since each phase can exist in a metastable state beyond the phase transition line and the spin flip takes place via an irreversible change of the orientation of the vector \mathbf{M} . The transition $\Phi\langle 110 \rangle \rightleftharpoons \Phi\langle 100 \rangle$, in the assumed approximation, is a specific hysteresis-free first-order transition, inasmuch as the regions of the existence of the phases $\Phi\langle 110 \rangle$ and $\Phi\langle 100 \rangle$ are contiguous but do not overlap, while the phase-stability-loss lines coincide with the phase-transition line.

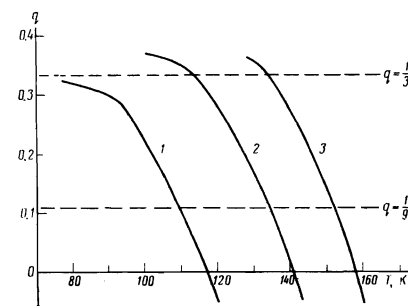


FIG. 4. Temperature dependence of the parameter $q = K_1/|K_2|$ for yttrium-terbium iron garnets. 1) $x = 0.10$; 2) $x = 0.26$; 3) $x = 0.50$.

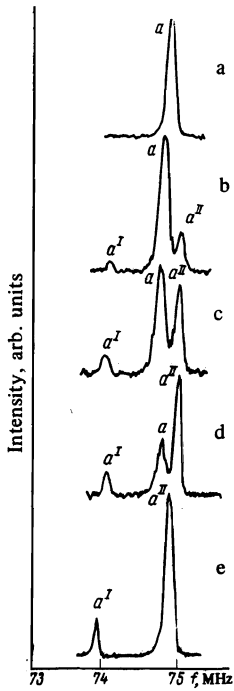


FIG. 5. NMR spectra of octahedral Fe^{3+} ions of the iron garnet $\text{Tb}_{0.1}\text{Y}_{2.9}\text{Fe}_5\text{O}_{12}$. Temperature, $^{\circ}\text{K}$: a) 104.2, b) 108.0, c) 108.7, d) 109.0, e) 115.0.

tion of the magnetization in the crystal can be obtained in this case by determining the orientation of the crystal relative to the external magnetic field. In this experimental geometry, all the results of the theoretical analysis for single-domain samples in the absence of an external magnetic field remain valid: it is only necessary to take into account the field dependence of the anisotropy constants. Investigations of orientation of single-crystal yttrium-terbium ferrite disks with $x = 0.10, 0.26,$ and 0.50 in a magnetic field as a function of the temperature make it possible to draw a conclusion that is important for further comparison with the NMR results, namely that, in full agreement with the theoretical phase diagram, the $\Phi\langle 100 \rangle \rightleftharpoons \Phi\langle 111 \rangle$ SF transition in a single-domain state remains a first-order hysteresis transition. The temperature width of the hysteresis loop is appreciable and is in satisfactory correlation with the width of the interval of the metastable states ($T\langle 100 \rangle - T\langle 111 \rangle$), determined from the theoretical phase diagram (relations (3)) and the experimental values of $K_1(T)$ and $K_2(T)$. For example, experiments on the orientation of the disk in a 5-kOe field yield for samples with $x = 0.50$ and 0.26 an approximate hysteresis-loop width 15 and 20° , respectively, close to the width of the interval of the metastable states, 24 and 27° , listed in the table. For a sample with $x = 0.10$, no transition from the $\Phi\langle 111 \rangle$ phase to the $\Phi\langle 100 \rangle$ phase take place even at the lowest measurement temperature (77°K), whereas the transition from the $\Phi\langle 100 \rangle$ phase into the $\Phi\langle 111 \rangle$ is completed. Such an "open" hysteresis loop agrees qualitatively with the temperature dependence of the anisotropy constants of this ferrite (Fig. 4, curve 1).

To determine the character of the transition in multidomain samples we registered the NMR spectra of Fe^{57} in local fields at the nuclei of the octahedral Fe^{3+} ions without applying an external magnetic field. The mea-

surements were performed near the expected transition temperatures listed in the table. Figure 5 shows by way of example the spectra of the nuclei in the volume of the domains of a single crystal with terbium content $x = 0.10$. At low temperatures (77 – 106°K) the spectrum is a narrow single resonance line (Fig. 5a). As was already considered in section 2, this shape of the NMR spectrum of the octahedral ions in iron garnet corresponds to magnetization directions in the domains along the crystallographic axes of the type $\langle 100 \rangle$ (line a in Fig. 1b). This result shows that only the $\Phi\langle 100 \rangle$ phases are realized at low temperatures. At high temperatures (111 – 200°K) the spectrum consists of two lines (Fig. 5e) with an intensity ratio close to $1:3$. This form of the spectrum agrees with the theoretically expected one of the magnetization in the domains is directed along axes of the $\langle 111 \rangle$ type (the lines a^I and a^{II} in Fig. 1b), i.e., only the $\Phi\langle 111 \rangle$ phases are realized at high temperatures.

Thus, both below and above the expected SF transition temperature in a multidomain sample of yttrium-terbium iron garnet, magnetic phases are observed corresponding to the phase diagram of the single-domain sample. However, in the 106 – 111°K , a superposition is observed of the two spectra considered above, which indicates the coexistence of the phases $\Phi\langle 100 \rangle$ and $\Phi\langle 111 \rangle$ (Figs. 5b–d). The intensities of the spectra of the phases $\Phi\langle 100 \rangle$ and $\Phi\langle 111 \rangle$ are smoothly redistributed with changing temperature, but no other lines appear, the magnitude of the splitting ($f_{a^{II}} - f_{a^I}$) does not change, and the line a does not change its position relative to the lines a^I and a^{II} . With increasing temperature, a monotonic shift of the resonance lines takes place (Fig. 6) towards lower frequencies without any anomalies whatever in the region of the SF transition, owing to the decrease of the average thermodynamic value of the spin of the octahedral Fe^{3+} ions or, equivalently, owing to the decrease of the sublattice magnetization. All these facts indicate unequivocally that the SF transition

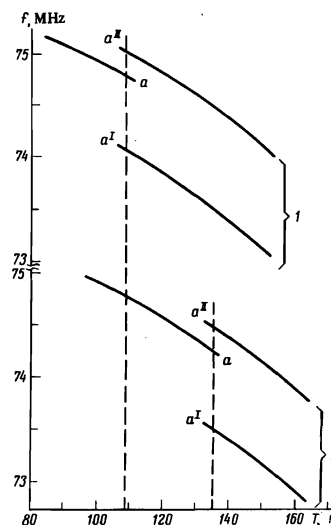


FIG. 6. NMR frequencies of octahedral Fe^{3+} ions in the vicinity of the spin-flip temperatures. The dashed lines show the positions of the spin-flip temperatures T_{sf} . 1) $x = 0.10$; 2) $x = 0.26$.

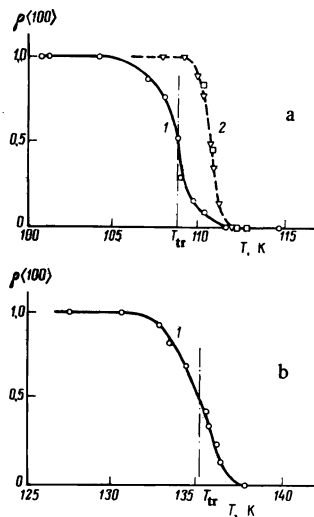


FIG. 7. Temperature dependences of the relative volume $\rho\langle 100 \rangle$ of the $\Phi\langle 100 \rangle$ phases from NMR data. Curves 1 were obtained for single crystals with natural faceting, and curve 2 for a sample cut from the peripheral part of the single crystal. The triangles and the squares represent points obtained as the temperature was raised and lowered, respectively, a) $x=0.10$; b) $x=0.26$.

$\Phi\langle 100 \rangle \rightleftharpoons \Phi\langle 111 \rangle$ in the multidomain state of the sample is of first order, and is accompanied by the coexistence of the magnetic phases $\Phi\langle 100 \rangle$ and $\Phi\langle 111 \rangle$ in a certain temperature interval in the vicinity of the transition temperature T_{tr} . A perfectly analogous transformation takes place in the spectra of single crystals with $x=0.26$ and 0.50 .

It must be specially emphasized that the NMR spectra recorded in two measurement cycles with rising and dropping temperature practically coincide, i.e., the NMR shows in a direct manner that the SF transition $\Phi\langle 100 \rangle \rightleftharpoons \Phi\langle 111 \rangle$ in a multidomain cubic ferrimagnet, although of first order, it follows a reversible course without a temperature hysteresis.

Figure 7 shows for the compositions with $x=0.10$ and 0.26 the temperature dependences of the relative volume of the $\Phi\langle 100 \rangle$ phases

$$\rho\langle 100 \rangle = \frac{V\langle 100 \rangle}{V\langle 100 \rangle + V\langle 111 \rangle}$$

which are identified with the ratio of the intensities of the resonance lines $I_a/(I_a + I_{aI} + I_{aII})$. Taking into account the sensitivity of the procedure, we assume the start and end of the transition to be the temperatures at which $\rho\langle 100 \rangle = 0.95$ and 0.05 , respectively. Inasmuch as in the case phase coexistence the concept of the transition temperature becomes arbitrary, we assume also that the temperature T_{tr} corresponds to $\rho\langle 100 \rangle = 0.5$. The table lists the transition temperature T_{tr} and the values of the temperature intervals of the phase coexistence, obtained by the NMR method. For single crystals with $x=0.5$, the presented data are approximate because of the deterioration and the line resolution in the spectra. Attention is called to the fact that in multidomain samples the reorientation temperatures T_{tr} obtained by direct measurements by the NMR method are

close to the temperature determined from the theoretical phase diagram in the single-domain case (the difference does not exceed $1.5-2^\circ$). The small difference between the transition temperatures can result from the influence of the residual uniaxial growth anisotropy or else as a result of the fact that NMR measurements were performed in a zero magnetic field, while the study of the phase diagram of the single-domains samples was made in a 5 -kOe field.

The data in the table reveal one more interesting feature of the SF transition in multidomain samples, namely, the temperature intervals of the coexistence of the magnetic phases $\Phi\langle 100 \rangle$ and $\Phi\langle 111 \rangle$, measured by the NMR method, are several times narrower than the metastable-state intervals determined both from the theoretical phase diagram and from experiments with freely suspended samples.

Thus, the experimental results offer convincing evidence of an appreciable influence of the domain structure of cubic ferrimagnets on the spin flip. The hysteresis-free character of the first-order SF phase transition in the multidomain state and the "smearing" of the transition, which manifests itself in the coexistence of magnetic phases in a certain temperature interval, are its most interesting features in comparison with the single-domain state.

The theoretical analysis of the influence of the domain structure of uniaxial magnets on SF transitions induced by an external magnetic field or by change of temperature has been the subject of many studies, for example^[10-13]. In the cubic-ferromagnet case of interest to us, this question was considered in^[1]. The Landau-Lifshitz method used in this investigation to calculate the distribution of the magnetization in an oscillated domain wall makes it possible to explain qualitatively the singularities of the spin-flip reorientation described above for the multidomain state, but does not make it possible to estimate the temperature interval of the coexistence of the magnetic phases. As will be shown below, such an estimate can be obtained by using Shirobokov's method,^[14] which deals with one-dimensional periodic domain structures. Inasmuch as the same differential equations are used in both methods (the Euler equations of the variational problem for a system with magnetic inhomogeneities and cubic magnetic anisotropy), but with different boundary conditions, we shall make use of the principal equations of^[11] without detailed explanations.

The first integral of Euler's equations takes the form

$$\left(\frac{d\theta}{d\xi}\right)^2 + \sin^2\theta \left(\frac{d\varphi}{d\xi}\right)^2 - F_A(\theta, \varphi) = E = \text{const.} \quad (5)$$

Terbium content, x	Results obtained from the theoretical relations (3) and (4) and from the experimental values of $K_1(T)$ and $K_2(T)$ at $H=5$ kOe.				Results of NMR experiments, $H=0$	
	$T\langle 100 \rangle$, K	$T\langle 111 \rangle$, K	T_{tr} , K	Width of interval of metastable states, deg	T_{tr} , K	Width of phase coexistence interval, deg
0.10	117	—	110	>40	108.8	5
0.26	141	134	134	27	135.2	4.5
0.50	158	134	152	24	150	6

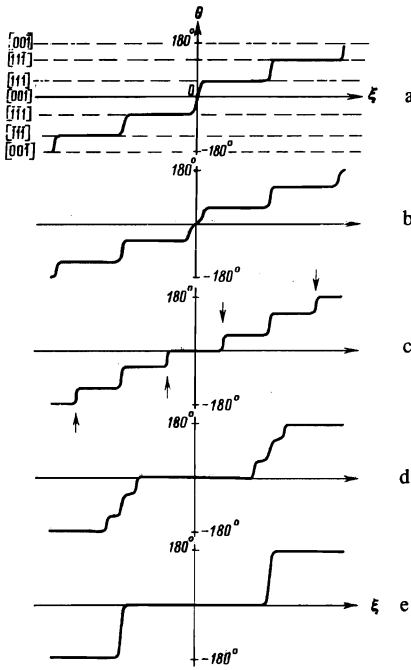


FIG. 8. Schematic representation of the behavior of the domain structure in the SF transition $\Phi\langle 100\rangle \rightleftharpoons \Phi\langle 111\rangle$. The arrows show the 55° walls separating the domains of the phases $\Phi\langle 100\rangle$ and $\Phi\langle 111\rangle$. The dimensions of the domains and of the domain walls are arbitrary. a) $q \leq 0$; b) $0 < q < 1/9$; c) $q = 1/9$; d) $1/9 < q < 1/3$; e) $q \geq 1/3$.

Here $\theta(\xi)$ and $\varphi(\xi)$ are the polar and azimuthal angles of the vector \mathbf{M} ; $\xi = x(A/|K_2|)^{-1/2}$ is the dimensionless coordinate;

$$\bar{F}_A = F_A / |K_2| = 1/4 q \sin^2 2\theta + 1/4 [q - \cos^2 \theta] \sin^4 \theta \sin^2 2\varphi$$

is the energy density of the cubic anisotropy in the case $K_2 < 0$ of interest to us, A is the Landau-Lifshitz exchange rigidity constant; E is an integration constant.

In the planar-wall model ($\varphi = \text{const}$), two groups of solutions are possible^[1] with $\varphi = n\pi/2$ and $\varphi = (2n+1)\pi/4$, which correspond to rotation of \mathbf{M} with one degree of freedom (θ) in planes of the type $\{100\}$ and $\{110\}$, respectively. Just as in^[1], we consider the case of rotation of \mathbf{M} in planes of the $\{110\}$ type. Then Eq. (5) is transformed into

$$\frac{d\theta}{d\xi} = \pm \{1/4 q \sin^2 2\theta + 1/4 [q - \cos^2 \theta] \sin^4 \theta + E\}^{1/2}. \quad (6)$$

The integration constant E can be represented in the form of two terms. One of them corresponds to a separatrix solution in the case of periodic solutions (isolated domain wall), and the other term, designated $\varepsilon(q) > 0$, takes into account the small deviation from the separatrix solution in the case of periodic solutions. It is easy to show that

$$E = \begin{cases} (1/27 - 1/3 q) + \varepsilon(q) & (0 \leq q \leq 1/9); \\ E = \varepsilon(q) & (1/9 \leq q \leq 1/3). \end{cases} \quad (7)$$

Direct calculation of the function $\theta(\xi)$ from (6) at an arbitrary value of q entails certain difficulties. Nevertheless, the influence of the domain structure on the spin flip can be clearly illustrated with the aid of the

phase portrait of the system, i.e., the dependence of $d\theta/d\xi$ on θ , at $\varepsilon = 0$ (see Fig. 2 of^[1]). If $q < 0$, then $d\theta/d\xi$ takes on zero values at θ equal to $\pm 55^\circ$ and $\pm 125^\circ$. So long as the angle θ remains quite close to these values, the derivative $d\theta/d\xi$ is small, i.e., changes little as a function of ξ . This means that there are realized four types of domains in which the magnetization is parallel to one of the four possible directions of the $\langle 111\rangle$ type in a plane of the $\{110\}$ type (the $\Phi\langle 111\rangle$ phase), and two type of domain walls are possible, 110° -degree domains and 70° -degree domains. Figure 8a shows schematically a plot of $\theta(\xi)$ at $q < 0$, within the limits of one period, for a periodic solution whose phase portrait is close to the considered phase portrait of the separatrix solution. When q increases from 0 to $1/9$, the value of $d\theta/d\xi$ at $\theta = 0$ and $\theta = \pi$ decreases, corresponding to the appearance of gently-sloping sections of the plot of $\theta(\xi)$ (Fig. 8b), which can be regarded as "nuclei" of new $\Phi\langle 100\rangle$ phases. As q approaches the value $1/9$, the width of the 100° -degree domain wall increases on account of these sections. At $q = 1/9$, $d\theta/d\xi$ on the phase portrait of the system assumes zero values at the points $\theta = 0, \pm 55, \pm 125, \text{ and } \pm 180^\circ$. This means that the 110° -degree wall splits into two 55° -degree walls (shown by arrows in Fig. 8c), between which are located the domains of the $\Phi\langle 100\rangle$ phases. At $1/9 < q < 1/3$ (Fig. 8d), the domains of the $\Phi\langle 111\rangle$ phases decrease and only the phases $\Phi\langle 100\rangle$ are realized with further increase of q (Fig. 8e).

This qualitative analysis shows that the SF transition $\Phi\langle 100\rangle \rightleftharpoons \Phi\langle 111\rangle$ proceeds in the assumed model via a continuous reversible growth of the new phase from unique "nuclei," which are the walls between the domains of the old phase. The transition is of first order only in the sense that only discrete directions of the magnetization along the axes of the type $\langle 111\rangle$ and $\langle 100\rangle$ are possible in the equilibrium domains. However, the change of the direction of the magnetic moment at a concrete point proceeds not jumpwise, but via a smooth rotation as the 55° -degree wall passes through this point during the course of the change of temperature. It is obvious that this transition has no hysteresis, as is indeed observed experimentally by the NMR method in the multidomain state of the samples. In addition, the presented qualitative analysis confirms in principle the possibility of coexistence of magnetic phases near a temperature satisfying the condition $q(T_{tr}) = 1/9$.

Let us compare the experimentally observed temperature range of the coexistence of the phases $\Phi\langle 111\rangle$ and $\Phi\langle 100\rangle$ (see the table) with the range calculated in the assumed model. To this end, we calculate the ratio of the volumes of the domains of the phases $\Phi\langle 100\rangle$ and $\Phi\langle 111\rangle$ within one period of the domain structure near $q = 1/9$, putting $q(T) = 1/9 + \Delta q(T)$. Discarding the contributions that are small in comparison with the period of the domain structure, we obtain from (6), taking (7) into account, the overall dimensions of the domains of the phases $\Phi\langle 100\rangle$ and $\Phi\langle 111\rangle$:

$$\left. \begin{aligned} D\langle 100\rangle &= -6 \ln[\varepsilon(\Delta q)^{-1/3} \Delta q] \\ D\langle 111\rangle &= -6\sqrt{3} \ln \varepsilon(\Delta q) \end{aligned} \right\} \Delta q < 0,$$

$$\left. \begin{aligned} D\langle 100 \rangle &= -6 \ln \varepsilon(\Delta q) \\ D\langle 111 \rangle &= -6\sqrt{3} \ln[\varepsilon(\Delta q) + \frac{1}{3}\Delta q] \end{aligned} \right\}, \quad \Delta q > 0. \quad (8)$$

The integration constant $\varepsilon(\Delta q)$ is calculated from the specified period of the domain structure^[14]:

$$\Delta(A/|K_2|)^{-1/2} \approx D\langle 100 \rangle + D\langle 111 \rangle. \quad (9)$$

The period of the domain structure can be determined, in principle, by starting from the specified dimensions and shape of the sample, for example, for a plate of given thickness. For the case of multiaxial (cubic) crystals, a construction of a domain structure with minimum energy seems to present great difficulties. Therefore, in our opinion, it is rational to use for estimates the experimental values of the periods of planar domain structures in iron garnets. In addition, we shall assume that the period Δ remains constant in the reorientation region. The basis for such an assumption is the fact that although the constant $K_1(T)$ goes through zero in the region of the transition, the second anisotropy constant remains large: $|K_2| \approx 40 \times 10^3 \text{ erg/cm}^3$. In other words, we assume that the redistribution of the volumes of the domains proceeds with conservation of the period of the domain structure; the dimensions of the domains of the $\Phi(100)$ phases increase at the expense of the decrease of the dimensions of the domains of the $\Phi(111)$ phases (and vice versa).

Using the data of^[15-19], we assume $\Delta \approx 5 \times 10^{-3} \text{ cm}$ and $A = 4.4 \times 10^{-7} \text{ erg/cm}$. Then

$$\Delta(A/|K_2|)^{-1/2} \approx 1.5 \cdot 10^2.$$

The solution of the transcendental equations (9) and (8) with this quantity taken into account makes it possible to calculate $\varepsilon(\Delta q)$ and then determine the dependence, of interest to us, of the relative volume of the $\Phi(100)$ phases:

$$\rho\langle 100 \rangle(\Delta q) = \frac{D\langle 100 \rangle}{D\langle 100 \rangle + D\langle 111 \rangle}$$

The calculations show that $\rho\langle 100 \rangle = 0.366$ at $\Delta q = 0$, and the assumed interval of reorientation between $\rho\langle 100 \rangle = 0.05$ and $\rho\langle 100 \rangle = 0.95$ corresponds to a deviation of q from the value $1/9$ by an amount $\Delta q \approx 2.2 \times 10^{-3}$. Taking into account the slope of the function $q(T)$ at $q = 1/9$ (Fig. 4), we arrive at the conclusion that the calculated width of the temperature interval of the reorientation is approximately 0.5 degree. On the other hand, if the reorientation limits are assumed to be the values $\rho\langle 100 \rangle = 0.1$ and 0.9, then the reorientation temperature interval amounts to only 10^{-4} deg. These results signify that the phases $\Phi(100)$ and $\Phi(111)$ coexist in comparable volumes only in the immediate vicinity of the transition temperature, determined by the relation $q(T_{tr}) = 1/9$, and consequently coinciding with the theoretical transition temperature in the single-domain case. The effect of redistribution of the volumes of the phases in defect-free samples takes place in a very narrow temperature interval, i. e., practically jumpwise, so that the phase diagram in the multidomain state takes the form shown in Fig. 3b.

The experimental data (see the table) confirm the theoretical conclusion that the temperature of the tran-

sition into the multidomain state coincides with the temperature determined by the theoretical phase diagram of the single-domain sample. However, the observed width of the phase coexistence interval contradicts the theoretical estimate. We can name three principal causes of this disparity.

1. Local deviations of the anisotropy constants from the mean values over the crystal should lead to an inhomogeneous evolution of the SF phase transition. From this point of view, inhomogeneities of the chemical composition can play an essential role, namely, inhomogeneities of the distribution of the Tb^{3+} ions. Estimates show that an inhomogeneity of approximately 20% of the terbium content can explain the observed smearing of the transition. According to x-ray structure investigations,^[8] in bulky single-crystal mixed garnets the inhomogeneities of the composition are of the order of 10-15%, especially in the internal parts of the crystals. These values of the inhomogeneity can almost completely explain the observed smearing of the transition. To verify this assumption, control measurements were made with a sample having linear dimensions $\sim 3 \text{ mm}$, cut from the periphery of a single crystal with dimensions $\sim 2 \text{ cm}$. The results of the measurements (dashed curve of Fig. 7a) show that the interval of the phase coexistence has narrowed down to 2° , i. e., by a factor 2.5. Thus, the inhomogeneities of the composition seem to be among the principal causes of the broadening of the transition.

2. Inhomogeneous internal stresses can be of great significance. A rough estimate shows that to explain the smearing of the transition of the transition in single crystals with $x = 0.26$ it is necessary to assume the presence of inhomogeneous stresses on the order of 10^2 kg/cm^2 . It appears that long-range strongly inhomogeneous stress fields of single dislocations and of their clusters play an important role and induce local magnetic anisotropy. In^[20], for example, the inhomogeneity of the distribution of the magnetization vectors in a field of dislocation stresses in a multidomain yttrium iron garnet sample was clearly demonstrated.

3. Inasmuch as an appreciable displacement of the domain walls should take place in the case of spin flip in samples with domain structure, a definite role can be played also by various effects that block the motion of the domain wall.

It should be noted that the width of the smearing interval of a first-order SF transition can thus serve as a certain integral criterion of the perfection of cubic ferrimagnets.

The authors thank K. P. Belov for interest in the work, V. G. Bar'yakhtar and A. K. Zvezdin for useful discussions of the results, and also B. V. Mill' for consultations on the single-crystal growth.

¹⁾A clear example of smooth transformation of the NMR spectra in the case of a second-order SF transition is provided by the investigation in^[6].

- ¹K. P. Belov, A. K. Zvezdin, R. Z. Levitin, A. S. Markosyan, B. V. Mill', A. A. Mukhin, and A. P. Perov, *Zh. Eksp. Teor. Fiz.* **68**, 1189 (1975) [*Sov. Phys. JETP* **41**, 590 (1975)].
- ²V. D. Doroshev, S. F. Ivanov, M. M. Koftun, and V. M. Selez'ob, *Dopovidi AN URSSR*, No. 1, 68 (1973).
- ³E. A. Turov and M. P. Petrov, *Yaderniy magnitnyy rezonans v ferro- i antiferromagnetnikakh* (Nuclear Magnetic Resonance in Ferro- and Antiferromagnets), Nauka, 1969.
- ⁴R. L. Streever and P. J. Caplan, *Phys. Rev. [B]* **4**, 2881 (1971).
- ⁵C. Robert and F. Hartmann-Boutron, *J. Phys. Radium* **23**, 574 (1962).
- ⁶V. G. Bar'yakhtar, V. A. Klochan, N. M. Kovtun, and E. E. Solov'ev, *Fiz. Tverd. Tela* **16**, 2058 (1974) [*Sov. Phys. Solid State* **16**, 1236 (1975)].
- ⁷K. P. Belov, A. K. Gapeev, R. Z. Levitin, A. S. Markosyan, and Yu. F. Popov, *Zh. Eksp. Teor. Fiz.* **68**, 241 (1975) [*Sov. Phys. JETP* **41**, 117 (1975)].
- ⁸A. S. Markosyan, Author's abstract of dissertation for the degree of Candidate of Physical and Mathematical Sciences, Moscow State University, 1975.
- ⁹V. G. Demidov, A. K. Zvezdin, R. Z. Levitin, A. S. Markosyan, and A. I. Popov, *Fiz. Tverd. Tela* **16**, 2114 (1974) [*Sov. Phys. Solid State* **16**, 1379 (1975)].
- ¹⁰V. G. Bar'yakhtar, A. E. Borovik, and V. A. Popov, *Pis'ma Zh. Eksp. Teor. Fiz.* **9**, 634 (1969) [*JETP Lett.* **9**, 391 (1969)].
- ¹¹V. G. Bar'yakhtar, A. E. Borovik, V. A. Popov, and E. P. Stefanovskii, *Zh. Eksp. Teor. Fiz.* **59**, 1299 (1970) [*Sov. Phys. JETP* **32**, 709 (1971)].
- ¹²A. I. Mitsek, N. P. Kolmakova, and P. F. Gaïdanskii, *Fiz. Tverd. Tela* **11**, 1258 (1969) [*Sov. Phys. Solid State* **11**, 1021 (1969)].
- ¹³A. I. Mitsek and P. F. Gaïdanskii, *Phys. Status Solidi [a]* **4**, 319 (1971).
- ¹⁴M. Shirobokov, *Zh. Eksp. Teor. Fiz.* **15**, 57 (1945).
- ¹⁵J. F. Dillon, *J. Appl. Phys.* **29**, 539 (1968).
- ¹⁶V. D. Dylgerov and A. I. Drokin, *Kristallografiya* **5**, 945 (1960) [*Sov. Phys. Crystallogr.* **5**, 900 (1961)].
- ¹⁷J. R. Patel, K. A. Jackson, and J. F. Dillon, *J. Appl. Phys.* **39**, 3767 (1968).
- ¹⁸J. E. Kunzler, L. R. Walker, and J. K. Galt, *Phys. Rev.* **119**, 1609 (1960).
- ¹⁹S. S. Shinozaki, *Phys. Rev.* **122**, 388 (1961).
- ²⁰V. K. Vlasko-Vlasov, L. M. Dedukh, and V. I. Nikitenko, *Zh. Eksp. Teor. Fiz.* **65**, 376 (1973) [*Sov. Phys. JETP* **38**, 184 (1974)].

Translated by J. G. Adashko

Equivalent noncollinear structures in the cubic ferrimagnet GdIG induced by a magnetic field

S. L. Gnatchenko and N. F. Kharchenko

Physico-technical Institute of Low Temperatures, Ukrainian Academy of Sciences

(Submitted October 9, 1975)

Zh. Eksp. Teor. Fiz. **70**, 1379-1393 (April 1976)

Fracture of GdIG sublattices near T_c is studied by means of the Faraday magneto-optical effect. A transverse experimental geometry is used, in which the light-propagation vector \mathbf{k} is perpendicular to \mathbf{H} . The coexistence of noncollinear equivalent magnetic structures (magnetic twins) is observed visually. The magnetic diagrams of the GdIG states are plotted on the basis of the observations for the cases $\mathbf{H} \parallel [100]$ and $\mathbf{H} \parallel [111]$. They are in satisfactory agreement with calculations performed within the framework of the molecular-field approximation with allowance for the GdIG three-sublattice structure and cubic anisotropy. It is suggested that the tail observed on the $\Phi(T)$ curve with increasing distance from the phase-transition line in the case of $\mathbf{H} \parallel [100]$ is due to microscopic defects of the sample and is similar to the tail of the technical-magnetization curve at saturation.

PACS numbers: 75.25.+z, 75.30.Gw, 78.20.Ls

A sufficiently strong field applied to a collinear ferrimagnet upsets the parallelism of its sublattices (see^[1], where references to earlier work are given). For a number of reasons (stratification near first-order phase transitions, the presence of several equivalent directions), the resultant noncollinear structure cannot be homogeneous. Visual observation of an inhomogeneous noncollinear magnetic structure of rare-earth iron garnets was reported in^[2-5]. The results of the investigation of the stratification of the magnetic phases in the vicinities of first-order orientational transitions in gadolinium iron garnets were discussed in^[4,5]. In this paper we investigate the twinning of the field-induced magnetic noncollinear structure of a gadolinium iron garnet when the magnetic field is ordered along its high-order symmetry axes.

METHODOLOGICAL REMARKS

The experimental method used was based on the magneto-optical rotation of the polarization plane whereby, owing to the significantly different partial contributions of the individual sublattices of the GdIG, it becomes possible to determine the angle between the magnetic moment of the optically active sublattice and the light-propagation direction. We used a transverse experimental geometry, in which the light-propagation direction \mathbf{k} was perpendicular to the magnetic field \mathbf{H} . At the employed field strengths, the angles between the magnetic moments of the a and d sublattices differ very little from 180° , and, neglecting the small contributions to the Faraday rotation of the GdIG, we can write